Effect of the surface states of different transition-metal substrates on a Cs overlayer

Ru-qian Wu
Laboratory for Surface Physics, Institute of Physics, Academia Sinica, P.O. Box 603, Beijing 100 080, China

Ding-sheng Wang
Chinese Center of Advanced Science and Technology (World Laboratory), P.O. Box 8730, Beijing 100 080, China and Laboratory for Surface Physics, Institute of Physics, Academia Sinica, P.O. Box 603, Beijing 100 080, China

(Received 24 July 1989; revised manuscript received 9 February 1990)

The linear augmented-plane-wave method is applied within the jellium-slab model to investigate the submonolayer cesiated (001) surfaces of Ta, W, Ir, Pt, Au, Ni, and Cu. At lower coverages, it is an ionic-adsorption regime in which the alkali-metal adlayer donates its electrons to the most influential surface state of the substrate. The characteristic coverage N_m, which marks the end of the ionic adsorption and is a measure of the ability of the most influential surface band of the substrate to hold extra electrons, decreases with increasing number of d electrons in the substrate atom. At higher coverages, however, the dipole moment p of the adsorption layer decreases rapidly, and in this polarized-metallic regime adsorption electrons are depolarized mainly by the Coulombic effect within the adlayer. The work-function minimum (0.5 eV) and the work function at the monolayer coverage (1.8 eV) are independent of the choice of substrate.

I. INTRODUCTION

The electronic properties of a chemisorption system consisting of an alkali-metal overlayer and a transition-metal substrate have been extensively studied with increasing interest since the pioneering works of Kingdon and Langmuir.[1-10] Experimentally, various properties, including flicker noise power, binding energy of the surface state of the substrate, work function, thermal desorption energy, electron energy-loss peak, and activation energy for parallel immigration, etc., are investigated with respect to the alkali-metal coverage. Dramatically, the coverage dependences of all these quantities suggest that the whole submonolayer coverage can be divided into two regimes in which adlayer-substrate interaction has different properties, i.e., an ionic and a neutral metallic regime (sometimes referred as a Mott transition). The coverage related to the work-function minimum ($N_{\min}$) is usually taken as the critical point.

In order to clarify the physical background of these interesting facts, theoretical studies have to take both localized surface states of transition-metal substrates and continuous coverage variance of alkali-metal overlayers into consideration. By solving the one-dimensional Kohn-Sham equation self-consistently on a model geometry treating both the adlayer and the substrate as jellium metals, Lang found that the work-function minimum is connected with the change of the distribution character of adsorption electrons.[6] At very low coverage, the adsorption electrons concentrate toward the substrate, which causes a rapid initial decrease of the work function. With growing coverage, however, the center of the distribution of the adsorption electrons moves away from the interface. The work-function minimum occurs when the decrease of the charge transfer is balanced by the increase of coverage. Very recently, Ishida *et al.* investigated the adsorption of a submonolayer sodium lattice on a jellium surface.[9] They stated that at the lower coverage ($<\frac{1}{3}$ monolayer), the bonding electrons between the adatoms and the substrate are mainly contributed by sodium adatoms (ionic interaction). At the higher coverage, however, the bonding electrons (with almost the same amount as at the lower coverage) come from both the substrate and the adatoms (covalent interaction). Nevertheless, since the d-like surface states of transition-metal surfaces can be hardly taken into account in these jellium substrate approaches, the physical background of the adsorption phenomenon is still unclear. Wimmer *et al.*, on the other hand, carried out very accurate numerical full-potential linear augmented-plane-wave (FLAPW) calculations to study the monolayer cesiated W(001) and Mo(001) surfaces. They treated both the adsorbate and the substrate by atomic layers.[7,8] As the result, 6s valence states of cesium adatoms interact with the known $\bar{\Gamma}\, d_{z^2}$ surface state (SS) of the W(001) [or Mo(001)] substrate strongly and form a covalent-metallic bond. The so-caused rearrangement of the adsorption electrons diminishes the surface Coulombic barrier (or the work function) by about 2.0 eV. They also reported that at the half-monolayer cesiation, the interaction and charge transfer, etc., have already exhibited similar characteristics as those at the monolayer cesiation.[8] Unfortunately, because two-dimensional translation periodicity in the film plane is a prerequisite in this type of atomic slab calculation, it is obviously impossible to investigate the coverage dependence of alkali-metal chemisorption processes this way.

In our recent study, chemisorption systems consisting of various submonolayer alkali-metal adsorbates on a W(001) surface are well described by using the jellium-

slab model and the accurate linear augmented-plane-wave (LAPW) method.[11,12] It was found that the whole submonolayer adsorption is indeed divided by a critical coverage N_m into an ionic adsorption regime and a polarized-metallic adsorption regime. At the lower coverage ($N_a < N_m$, where N_a denotes the atomic density of adsorbates), the alkali-metal adlayer donates its electrons to the known $\bar{\Gamma}$ d_{z^2} SS of the W(001) substrate. This causes a plateau of the adsorption dipole moments $p(N_a)$ within the coverage range of $N_a < N_m = 0.18 \times 10^{15}$ cm^{-2} for all alkali-metal species (as shown in Fig. 7 of Ref. 12). At the higher coverage, by contrast, the adsorption electrons are drawn outward gradually by their intensified positive background and intend to form a neutral metallic bond within the adlayer. The $p(N_a)$ thereby decreases quickly with the increasing coverage. The demarcation $N_m = 0.18 \times 10^{15}$ cm^2 (corresponding to 0.18 adatoms or adsorption electrons per surface tungsten atom) depends merely on the character of the W(001) surface, and furthermore can be considered as the ability of the $\bar{\Gamma}$ d_{z^2} surface state of W(001) surface to hold extra additional electrons from the alkali-metal adlayer.

The success of the jellium-slab model is not unexpected. At the higher coverage (e.g., $> \frac{1}{3}$ monolayer), the distance between alkali-metal adatoms is close enough and their s states overlap considerably, so the adlayer can be well simulated by a jellium, of course. At the very low coverage, the alkali-metal adatoms will be almost entirely ionized. Therefore, even though the jellium simulation breaks down, it is still expected to give a correct description for planar averaged quantities, such as adsorption dipole moment and work function, etc.

In the present work, we extend this treatment to study other systems including cesiated (100) surfaces of Ta, W, Ir, Pt, Au, Cu, and Ni in order to investigate further the effect of different surface states. The computational details are presented in Sec. II. The adlayer-substrate interaction and the so-caused charge rearrangement are discussed separately for different substrates in Sec. III. The coverage dependences of the adsorption dipole moment p and the work function ϕ are given in Secs. IV and V, respectively. A brief summary and conclusion are presented in Sec. VI.

II. COMPUTATIONS

The jellium-slab model and the LAPW method modified for an accurate description of the jellium-vacuum region have been discussed thoroughly in Ref. 12. In the present work, all the substrates are simulated by a three-layer ideal atomic slab with the 2D structure parameters chosen according to relevant bcc or fcc transition-metal crystals, i.e., $a = 6.2214$ a.u. (Ta), 5.9798 a.u. (W), 5.1212 a.u. (Ir), 5.2345 a.u. (Pt), 5.4462 a.u. (Au), 4.7054 a.u. (Ni), and 4.8377 a.u. (Cu). Two pieces of jellium, which represent the Cs adlayers, cover on both sides of the substrate slab. The thickness of the jellium is set equal to the distance between the most densely packed lattice planes of the cesium crystal ($D = 8.08$ a.u.) and remains independent of the coverage N_a within the whole submonolayer adsorption range. The positive charge density in the jellium, nevertheless, changes with the coverage $\Theta = N_a / N_{\mathrm{ML}}$ as $\rho_+ = 0.001338\Theta$ (N_{ML} denotes the density of adsorbates at the monolayer coverage) in order to simulate the variation of the alkali-metal adatom density.

The three layers as used in the present calculation are not thick enough to give an accurate work-function value.[13] In fact, it will give a work function value about 0.8 eV larger than the accurate one for the W(001) surface.[11] The splitting of the surface states due to artificial surface-surface interaction is about 0.2 eV for the d surface states of the W(001) surface. However, in the following investigation of the coverage dependence, these effects are kept unchanged, so they should not influence the results and the physics given below.

LAPW calculations are carried out for these modeled adsorption systems with more than 50 symmetrized (with respect to z reflection) plane waves and three special $\mathbf{k}$ points in a $\frac{1}{8}$ irreducible portion of the two-dimensional (2D) Brillouin zone. Self-consistencies are assumed when the mean-square differences between the input and output potentials are less than 15 mRy.

III. ADLAYER-SUBSTRATE INTERACTION AND THE CHARGE REARRANGEMENT

A. Cs/Ta(001) and Cs/W(001) systems

In their LAPW calculation, Krakauer *et al.* found that though the band of the Ta(001) surface is approximately the same as that of the W(001) surface by shifting its Fermi level downward about 1.8 eV,[14] the $\bar{\Gamma}$ d_{z^2} surface state of the Ta(001) surface, however, still lies just below the E_f (-0.3 eV) because its occupation is very closely related to the surface barrier. It can therefore be assumed that the Ta(001) surface will influence the alkali-metal adlayer in the same way as does the W(001) surface. Experimentally, Soukiassian *et al.* confirmed the existence of the $\bar{\Gamma}$ d_{z^2} SS below the Fermi energy, and moreover, found that the coverage dependence of the energy of this SS of the Ta(001) surface on the Cs coverage is indeed very similar to that for the W(001) substrate by the normal-emission ARUPS investigation on the Cs/Ta(001) and Cs/W(001) systems.[5]

The present results of the layer projected density of states (DOS) of clean and cesiated Ta(001) surfaces are plotted in Fig. 1. The center layer projected DOS of the Ta(001) slab shows the bulk DOS character of the Ta crystal (distinct separation between bonding and antibonding parts) and is almost independent of the adsorption. This suggests that the three-layer slab is roughly thick enough to simulate the Ta(001) substrate. From curves of surface layer projected DOS [(b), (c), and (d), corresponding to the clean, half-monolayer cesiated and monolayer cesiated Ta(001) surfaces, respectively], it can be found that the peak for those $d_{xz} \pm d_{yz}$ surface resonances lying 0.5 eV below the E_F for the W(001) surface (see Fig. 2 of Ref. 12) is shifted to above the Fermi energy for the clean and cesiated Ta(001) surfaces (peaks in the

range of 0–1.0 eV). Furthermore, the $\bar{\Gamma}$ d_{z^2} surface state [the small peaks lying just below the E_F on curves (b), (c), and (d)] shifts its energy downward slightly as the Cs adlayer is being deposited, which reveals the influence of the alkali-metal adlayer on this SS.

The symmetrized Σ_1 band of surface states (with their projection in the surface layer greater than 75%) for the clean and full-monolayer cesiated Ta(001) surfaces is shown in Fig. 2. Clearly, as marked out by the arrow in panel (a), there exists a $\bar{\Gamma}$ d_{z^2} surface state 0.3 eV below the E_F. Away from the $\bar{\Gamma}$ point, this SS disperses downward slightly and loses its surface character quickly due to hybridizing with the bulk Δ_5 band. As shown by its single-state charge density in Fig. 3(a), the $\bar{\Gamma}$ d_{z^2} SS of the Ta(001) surface exhibits a large vacuum extension. It thus will interact with the *s*-like states of the Cs adlayer as strongly as for the W(001) substrate. Comparing the band structures of the monolayer cesiated and clean

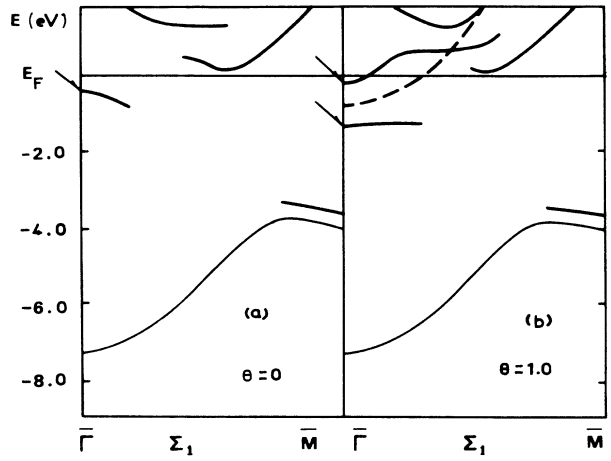

FIG. 2. The *z*-symmetric Σ_1 surface bands (projection in the surface layer greater than 75%) of the (a) clean Ta(001) surface and (b) the monolayer cesiated Ta(001) surface. The dashed line shows the dispersion of the jellium state ($m^*=m_e$). Arrows show the $\bar{\Gamma}$ d_{z^2} SS and its bonding and antibonding states.

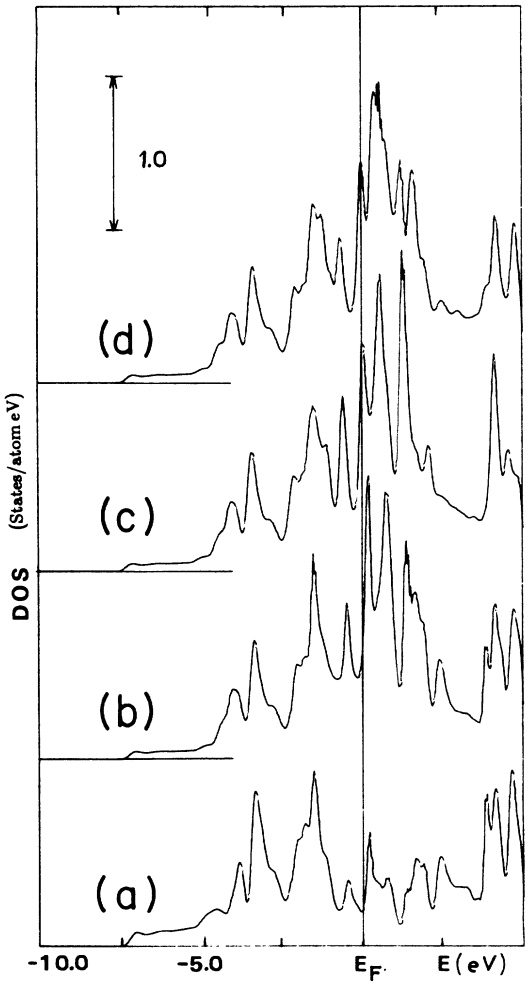

FIG. 1. Layer projected density of states of (a) the center Ta layer, (b) the surface Ta layer of the clean substrate, (c) the surface layer for the half-monolayer cesiated Ta(001) surface, (d) the monolayer cesiated Ta(001) surface. Units are states/eV per atom.

Ta(001) surfaces in Figs. 2(a) and 2(b), only the d_{z^2} surface band is perturbed remarkably at and out away from the $\bar{\Gamma}$ point. Other SS and SR bands, due to different spatial symmetry and less vacuum extension, scarcely change their energy position and dispersion when the Cs monolayer is deposited on. This suggests that as for the Cs/W(001) system, the Ta(001) surface influences an alkali-metal overlayer also mainly by this d_{z^2} SS. At the monolayer cesiated case, this SS mixes considerably with the jellium state of adlayer [dashed parabolic line in Fig. 2(b)]. The bonding state [marked by the lower arrow in Fig. 2(b)] contains a great deal of free-electron character, as shown in Fig. 3(b).

Figure 4(a) shows the difference of charge density of

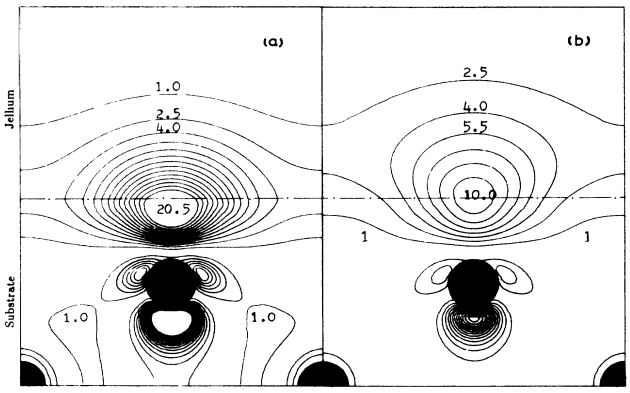

FIG. 3. Single-particle density of (a) the $\bar{\Gamma}$ d_{z^2} SS of the clean Ta(001) surface and (b) the bonding state of the $\bar{\Gamma}$ d_{z^2} SS with the jellium state of the monolayer cesiated Ta(001) surface. Contours are marked in units of 10^{-4} a.u.$^{-3}$ The area shown is on the vertical (110) plane through Ta atomic sites.

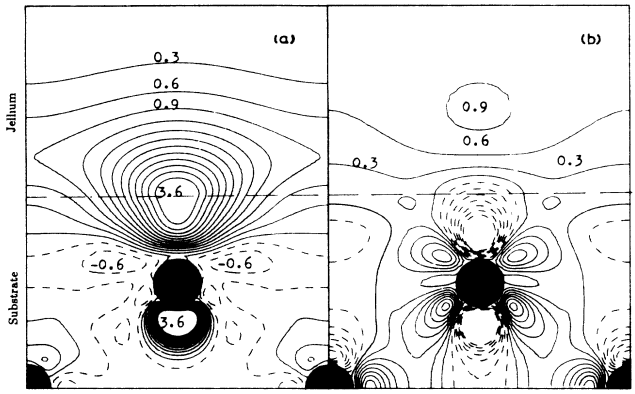

FIG. 4. Differences in the valence electron for the cesiated Ta(001) surface. (a) $\rho(\Theta=0.5)-\rho(\Theta=0)$, (b) $\rho(\Theta=1.0)-\rho(\Theta=0.5)$. Contours are marked in units of 10^{-4} a.u.$^{-3}$ The area shown is on the vertical (110) plane through Ta atomic sites.

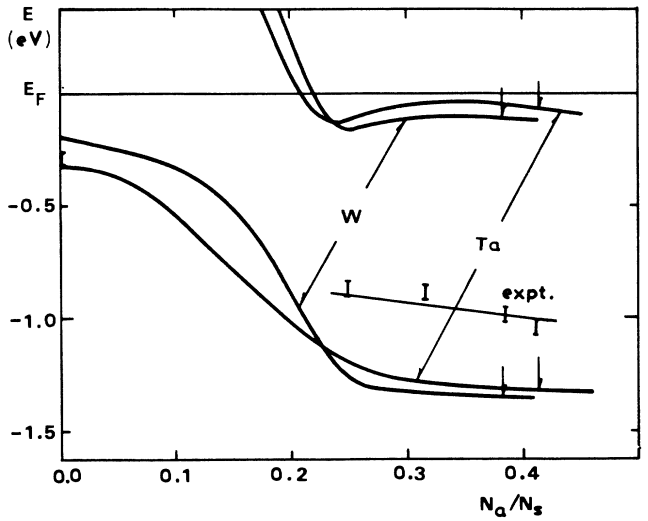

FIG. 5. Coverage dependences of the energies at the $\bar{\Gamma}$ point of bonding and antibonding bands between the $\bar{\Gamma}$ d_{z^2} SS of the substrate and the adlayer jellium state for the cesiated W(001) and Ta(001) surfaces. Experimental data (bars) are reproduced from Ref. 5 for the Cs/Ta(001) system. The coverage axis is scaled by the surface atomic density N_s of the corresponding substrate. Vertical arrows show the monolayer coverage.

$\rho(\Theta=0.5)-\rho(\Theta=0)$ for the Cs/Ta(001) system. It is noticeable that the redistribution pattern of adsorption electrons is very similar to the spatial distribution of the $\bar{\Gamma}$ d_{z^2} surface state of the substrate [shown in Fig. 3(a)]. That suggests an ionic adlayer-substrate interaction within the first half-monolayer adsorption, i.e., the Cs adlayer donates its electrons to fill the $\bar{\Gamma}$ d_{z^2} surface state of the Ta(001) substrate. At the higher coverage, as shown in Fig. 4(b) by $\rho(\Theta=1)-\rho(\Theta=0.5)$, the additional adsorption electrons distribute rather uniformly over their background region to form a metallic bond within the adlayer, because it becomes energy unfavorable to fill the SS of the substrate due to the Coulombic repulsion between stacked electrons and the intensified attraction from the positive background.

The energies at the $\bar{\Gamma}$ point of the interaction bonding and antibonding band between the $\bar{\Gamma}$ d_{z^2} SS and the adlayer jellium state for the Cs/W(001) and Cs/Ta(001) systems are shown in Fig. 5 with respect to the coverage (scaled by the surface atomic density N_s in order to emphasize the effect of the surface states of the substrate). In comparison, a related experimental result obtained from the normal-emission ARUPS for the Cs/Ta(001) system is also given[5] (denoted by bars). The SS lies 0.3 eV below the Fermi energy for the clean surface and is lowered to 1.3 eV for the monolayer cesiated Ta(001) surface, showing a good agreement with the relevant experimental result 0.3 and 1.1 eV. As shown in Fig. 5 of Ref. 12, the agreement for the W(001) substrate is also remarkable. This shows the validity of the jellium-slab model treatment. Furthermore, the antibonding state becomes lower than E_F and gets slightly occupied as the coverage grows larger than half-monolayer. This will enhance the interaction between alkali-metal adatoms, but will reduce the adlayer-substrate interaction. This can be assumed to be the reason why the desorption energy decreases at the higher coverage.[15]

B. The Cs/Ir(001) system

The singly symmetric [with respect to the z reflection and the (010) mirror plane] bands of surface states and resonances are shown in Figs. 6(a) and 6(b) for the clean and monolayer cesiated Ir(001) surfaces, respectively. In panel *a*, there are three surface SS and SR bands along

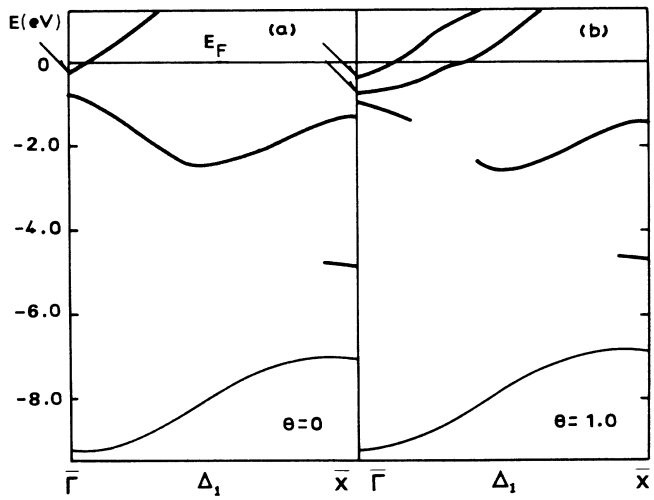

FIG. 6. The z-symmetric Δ_1 surface bands (projection in the surface layer greater than 75%) of (a) the clean Ir(001) surface and (b) the monolayer cesiated Ir(001) surface. Arrows show the SR1 and its bonding and antibonding states at the $\bar{\Gamma}$ point.

the Δ_1 line for the clean Ir(001) surface. Two are fully occupied: one lying 1–3 eV below the E_F possesses d_{xz} character, and the other, lying about 5 eV below the E_F, has a d_{z^2} symmetric property and shows its surface localization only near the $\bar{X}$ point. These two states, because of either symmetry or less vacuum extension, can hardly influence the Cs adlayer. Another surface resonance, which lies just below (0.2 eV) the E_F and is symmetric for all the C_{4v} operations at the $\bar{\Gamma}$ point, is thus expected to interact with the alkali-metal overlayer (this SR will be denoted by SR1 below). As seen from the surface band of the monolayer cesiated Ir(001) surface in Fig. 6(b), the SR1 band is disturbed noticeably by the Cs adsorption, but the former two bands are only slightly influenced in its surface projection by second-order effects (e.g., adsorption-induced rehybridization). From the single-state charge density in Fig. 7(a), it is shown that the SR1 mainly consists of the s- and p-like wave functions trapped near the surface region by the potential barrier. Therefore, the spatial distribution of the SR1 is rather sensitive to any variation of the surface environment. When the surface barrier is diminished by the alkali-metal adsorption, the SR1 will gradually extend its spatial range into the jellium-vacuum region. That is different from the $\bar{\Gamma}$ d_{z^2} SS of the W(001) and Ta(001) substrates, since this SS hardly changes its wave function with the alkali-metal adsorption. Subsequently, as shown in Fig. 7(b), the bonding state between the SR1 and the jellium state almost entirely loses the original character (in panel a) but mainly distributes over the jellium-vacuum region. The similarity of the density near the central layer in Figs. 7(a) and 7(b) shows that the influence of the jellium layer is indeed localized to the surface atom without appreciable influence even to the sublayer.

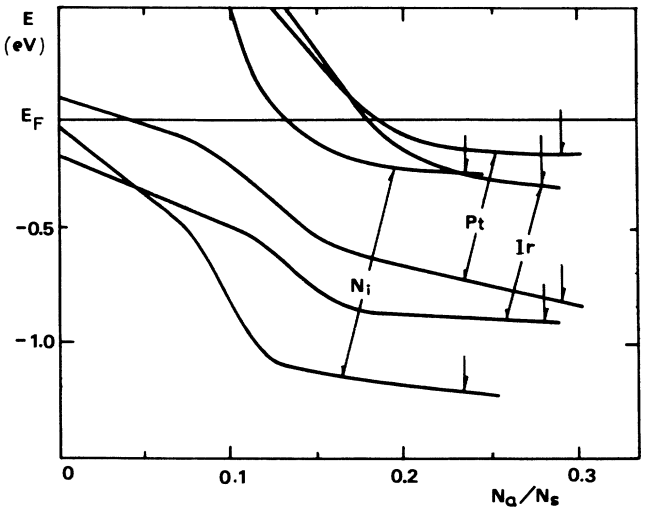

FIG. 8. Coverage dependences of the energies at the $\bar{\Gamma}$ point of bonding and antibonding bands between the SR1 of the substrate and the adlayer jellium state for the cesiated Ir(001), Pt(001), and Ni(001) surfaces. The coverage axis is scaled by the surface atomic density N_s of the corresponding substrate. Vertical arrows show the monolayer coverage.

In Fig. 8, the coverage dependences of the energies of the bonding and antibonding states generated by the SR1 and the jellium state at the $\bar{\Gamma}$ point for the Cs/Ir(001) system are shown. Because the DOS of the SR1 is small at the Fermi level (due to the strong dispersion across the E_F) and its spatial distribution changes with the absorption continuously, the energy of the bonding state decreases right from the initial alkali-metal deposition. It is lowered by 0.6 eV when $N_a/N_s=0.17$ (about 0.6 monolayer) and becomes saturated thereafter till the monolayer coverage.

Figure 9 presents the differences of the valence charge

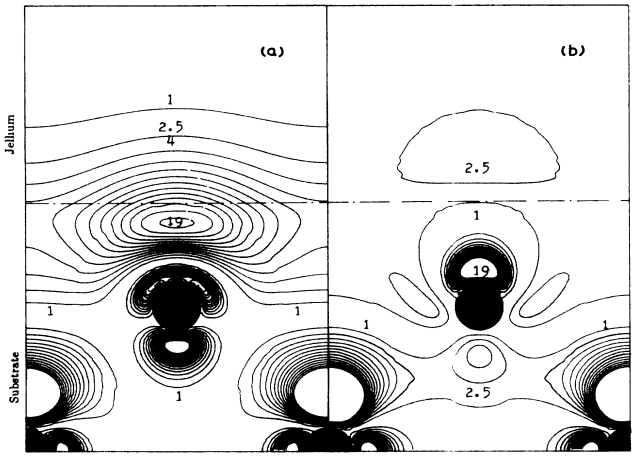

FIG. 7. Single-particle density of (a) the SR1 of the clean Ir(001) surface and (b) the bonding state of the SR1 with the jellium state of the monolayer cesiated Ir(001) surface. Contours are marked in units of 10^{-4} a.u.$^{-3}$ The area shown is on the vertical (100) plane through Ir atomic sites.

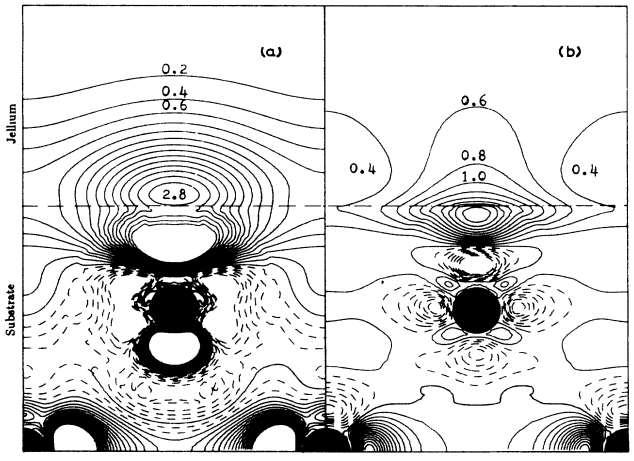

FIG. 9. Differences in the valence electron density for the cesiated Ir(001) surface. (a) $\rho(\Theta=0.45)-\rho(\Theta=0)$, (b) $\rho(\Theta=1.0)-\rho(\Theta=0.45)$. Contours are marked in units of 10^{-4} a.u.$^{-3}$ The area shown is on the vertical (100) plane through Ir atomic sites.

density for the Cs/Ir(001) system. Panel (a) is the difference of electron distribution $\rho(\Theta=0.45)-\rho(\Theta=0)$. Though the adsorption electrons are rearranged in a complicated way, they essentially are ionized by the SR1 of the Ir(001) substrate at the lower coverage. Due to the adsorption induced rehybridization, the interaction between the surface and the subsurface Ir layers is also slightly weakened. Detailed comparison of Figs. 9(a) and 7(a) reveals that the average center of the adsorption charge redistribution shifts slightly outward with respect to that of the SR1 of the clean Ir(001) surface. It can be referred to the sensitivity of the wave function of the SR1 to the adsorption induced modification in the surface environment. The charge difference of $\rho(\Theta=1)-\rho(\Theta=0.45)$ is presented in Fig. 9(b). The adsorption electrons rearrange almost uniformly over their positive background region at the higher coverage. That suggests, however, a polarized-metallic bond is formed in the adlayer, similar to what occurs in the Cs/W(001) and Cs/Ta(001) systems. Though the maximum of the electron density difference is on the transition metal side in the present Cs/Ir(001) case, different from W,[12] Ta [Fig. 4(b)], Pt [Fig. 11(b)], and Cu [Fig. 16(b)], it is not to be interpreted as ionization, because the dominant part of this charge difference is in the jellium region. However, it indicates that the hybridization of the localized d states with the metallic jellium states could be appreciable even in the high-density domain.

C. Cs/Pt(001) and Cs/Ni(001) systems

Ni and Pt surfaces with different orientations have been extensively investigated because of their importance in the catalysis and surface magnetism.[16–19] According to present results, the surface bands of the clean Ni(001) surface (without spin polarization) are qualitatively the same as those of the Pt(001) surface, and so is the effect on the Cs adlayer. Therefore, we concentrate our discussion mainly on one of them, namely, the Cs/Pt(001) system.

The Δ_1 SS and SR bands of the clean surface and the monolayer cesiated Pt(001) surface are shown in Figs. 10(a) and 10(b), respectively. Comparing Fig. 10 with Fig. 6, the surface bands of the Pt(001) (both clean and cesiated) are very similar to those of the Ir(001) surfaces. For instance, the two occupied SS and SR still remain, except their positions with respect to the Fermi level are rigidly moved downward by about 1 eV, and the d_{xz} SR loses its surface locality from the middle to the end of the Δ_1 line. Because of its sensitivity to the variation of the surface barrier, the SR1 does not change much in its position with respect to the Fermi level (lying 0.1 eV above the E_F at the $\bar{\Gamma}$ point). Consequently, as suggested by Fig. 10(b), the SR1 is also the main state of the Pt(001) surface influencing the alkali-metal overlayer.

In Fig. 8, the coverage dependences of the energies of the bonding and antibonding states at the $\bar{\Gamma}$ point generated by the SR1 and the adlayer jellium state for the Cs/Ni(001) and Pt(001) systems are plotted. At the monolayer coverage, the energy of the bonding state is lowered by 1.0 eV from that of the SR1 of the clean

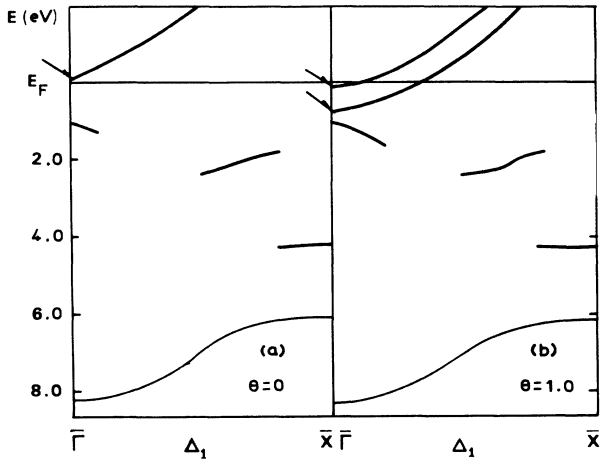

FIG. 10. The z-symmetric Δ_1 surface bands (projection in the surface layer greater than 75%) of (a) the clean Pt(001) surface and (b) the monolayer cesiated Pt(001) surface. Arrows show the SR1 and its bonding and antibonding states at the $\bar{\Gamma}$ point.

Pt(001) surface [1.2 eV for the Cs/Ni(001) system]. Corresponding experimental data are still absent to our knowledge.

Figure 11 presents the differences of the valence charge density for the Cs/Pt(001) system. Panel a is $\rho(\Theta=0.45)-\rho(\Theta=0)$. Similar to those systems discussed above, the adsorption electrons are ionized to the SR1 of the Pt(001) substrate at the lower coverage. At the higher coverage, however, these adsorption electrons intend to be distributed uniformly over the jellium region. Adsorption-induced rehybridization is also noticeable for the Cs/Pt(001) system. For example, the p_z state of the Pt surface atoms is weakened, but the d_{xy} state, making bonds between surface Pt atoms, is enhanced at the lower coverage.

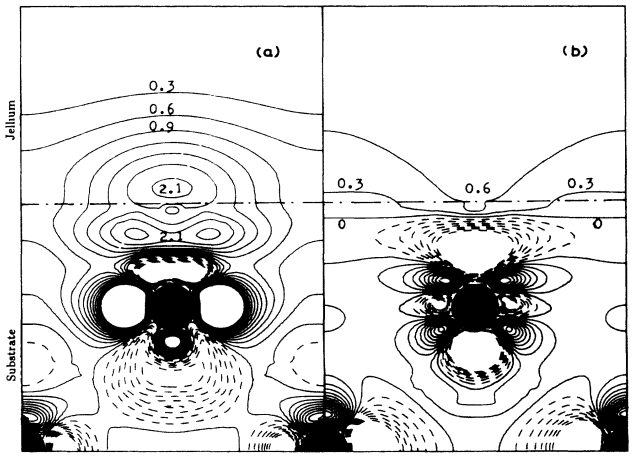

FIG. 11. Differences in the valence electron density for the cesiated Pt(001) surface. (a) $\rho(\Theta=0.45)-\rho(\Theta=0)$, (b) $\rho(\Theta=1.0)-\rho(\Theta=0.45)$. Contours are marked in units of 10^{-4} a.u.$^{-3}$ The area shown is on the vertical (100) plane through Pt atomic sites.

D. Cs/Cu(001) and Cs/Au(001) systems

Since the d bands of Cu and Au are already entirely filled, it is expected that the Cu(001) and Au(001) surfaces influence the alkali-metal adlayer in a way different from the Ta, W, Ir, Ni, and Pt(001) substrates. The surface bands of the Au(001) surface are qualitatively similar to those of the Cu(001), so we will mainly discuss the Cs/Cu(001) system.

Figure 12 shows the layer projected DOS for the clean and cesiated Cu(001) surfaces. The center layer projected DOS, as shown by curve (a), exhibits distinct bulk character and remains intact with respect to the Cs adsorption. This suggests that the three-layer slab is also reasonably good to simulate the noble metal Cu(001) surface, at least as far as the d bands are concerned. The d-band width is 3.5 eV, and the top of this band is 1.8 eV below the E_F according to present calculations, in good agreement with previous theoretical results.[20–22] Because the Cu atoms in the surface layer lose four neighbors, the d-band width of the clean surface layer [curve (b)] is greatly reduced, and its center of gravity evidently moves toward the top of the d band. More precisely, those high peaks on curve (b) can be explained by the induced Tamm surface states, because the average potential in the surface region is slightly more raised than in the bulk. Comparing the surface-layer projected DOS of the half-monolayer and monolayer cesiated Cu(001) surfaces [curves (c) and (d)] with curve (b), the adsorption-induced change on the DOS is not as manifested for the Cu substrate.

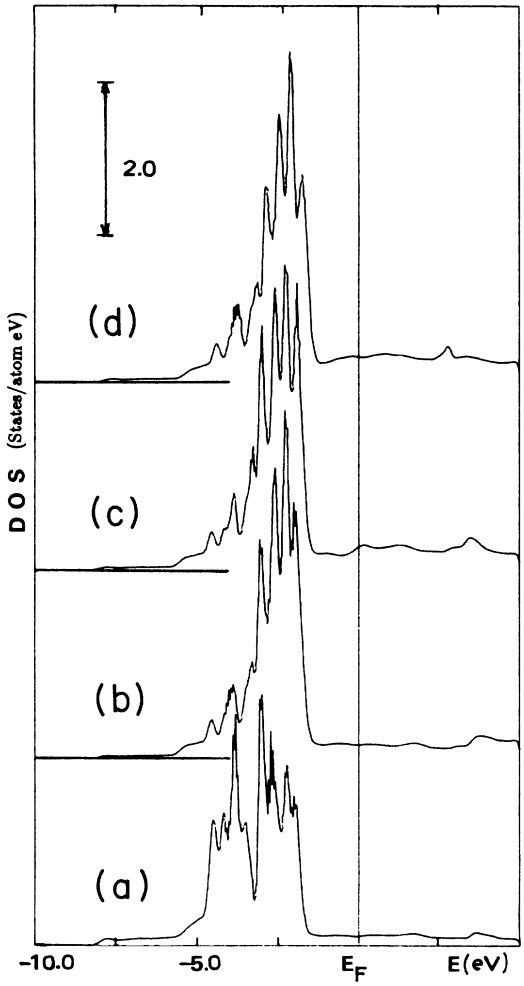

FIG. 12. Layer-projected density of states of (a) the center Cu layer, (b) the surface Cu layer of the clean substrate, (c) the surface layer for the half-monolayer cesiated Cu(001) surface, and (d) the monolayer cesiated Cu(001) surface. Units are states/eV per atom.

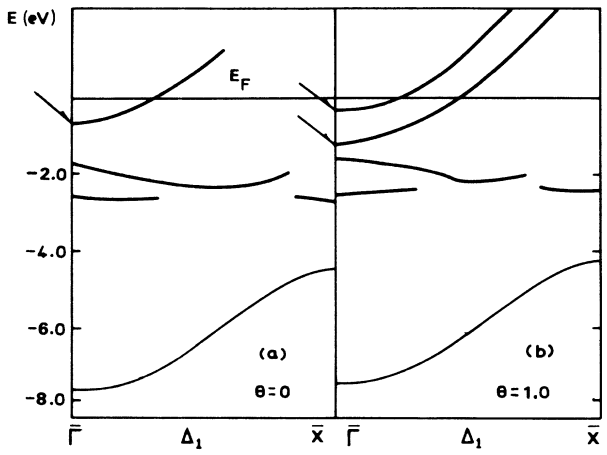

FIG. 13. The z-symmetric Δ_1 surface bands (projection in the surface layer greater than 75%) of (a) the clean Cu(001) surface and (b) the monolayer cesiated Cu(001) surface. Arrows show the SR1 and its bonding and antibonding states at the $\bar{\Gamma}$ point.

The Δ_1 surface bands of the clean and monolayer cesiated Cu(001) surfaces are shown in Figs. 13(a) and 13(b). In panel a, two fully occupied Tamm surface resonances can be found in the range of 2.0–3.0 eV below the Fermi energy, and a free-electron-like (with a parabolic $\mathbf{k}$ dispersion) SR band lies near the E_F (0.7 eV below the E_F at the $\bar{\Gamma}$ point). The high-lying SR, as shown by its single-state charge density profile in Fig. 14(a), is similar to the SR1 of the Ir and Pt(001) surfaces, except it has been partly filled. Because the two occupied SS and SR are far below the E_F in energy and, moreover, have less vacuum extension (backbonds), the SR1 is still the dominant state of the Cu(001) to interact with the Cs overlayer. This is clearly shown in Fig. 13(b), where only the SR1 band is obviously disturbed by the jellium state of the Cs monolayer. Since the SR1 of the substrate depends on the profile of the surface potential sensitively, the charge density of the bonding state of the monolayer cesiated Cu(001) surface [Fig. 14(b)] distributes mainly over the jellium-vacuum region without recognizable descent of the original SR1.

Figure 15 presents the coverage dependences of the energies of the bonding and antibonding states at the $\bar{\Gamma}$ point for the Cs/Cu(001) and the Cs/Au(001) systems. Within the submonolayer range, they show an obvious oscillation, different from that for the systems discussed

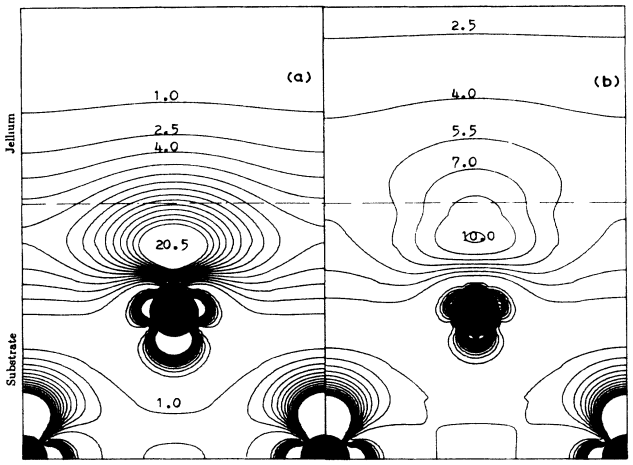

FIG. 14. Single-particle density of (a) the SR1 of the clean Cu(001) surface and (b) the bonding state of the SR1 with the jellium state of the monolayer cesiated Cu(001) surface. Contours are marked in units of 10^{-4} a.u.$^{-3}$. The area shown is on the vertical (100) plane through Cu atomic sites.

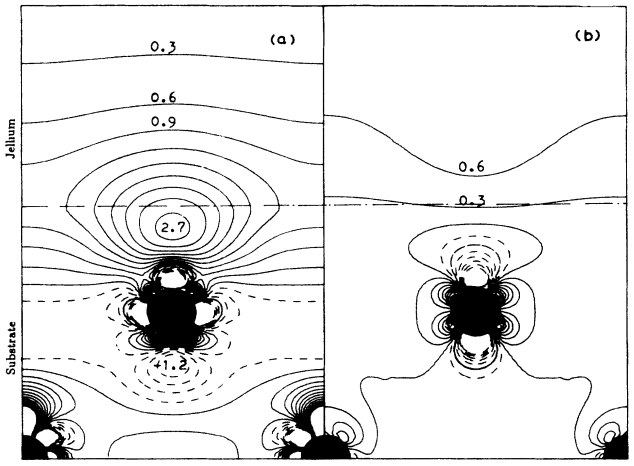

FIG. 16. Differences in the valence electron density for the cesiated Cu(001) surface. (a) $\rho(\Theta=0.45)-\rho(\Theta=0)$, (b) $\rho(\Theta=1.0)-\rho(\Theta=0.45)$. Contours are marked in units of 10^{-4} a.u.$^{-3}$. The area shown is on the vertical (100) plane through Cu atomic sites.

above. Since the three-layer slab used in our calculation is not thick enough to describe the itinerant s states, it is not certain that the oscillation behavior is a physical reality. For the Cs/Cu(001) system, the energy of the bonding state of the monolayer coverage is lowered by 0.4 eV from the position of the SR1 of the clean substrate. This agrees well with the relevant experimental value, also 0.4 eV, obtained from the Cs and Na/Cu(111) systems.[23]

The charge density of the Cs/Cu(001) system is given in Fig. 16. In panel (a), the spatial distribution profile of $\rho(\Theta=0.45)-\rho(\Theta=0)$ is obviously analogous to that of the SR1 of the clean Cu(001) substrate [Fig. 14(a)]. So even for the noble-metal substrates, the adsorption electrons are still ionized to fill the most influential SS (or SR) of the substrate. Careful comparison between Fig. 16(a) and Fig. 14(a) reveals that the center of gravity of the former is slightly shifted outward. That is because the average center of the SR1 of the Cu(001) surface moves outward gradually when the surface potential barrier is diminished by the absorption. In Fig. 16(b), the adsorption electrons fill its background very uniformly, and a metallic bond in the alkali-metal overlayer is gradually established. Furthermore, as obviously suggested by Figs. 16(a) and 16(b), the adsorption-induced rehybridization is not as distinct as that which occurred in the Cs/Ir(001) and Cs/Pt(001) systems, since the SR1 of the Cu(001) lies far from the d band.

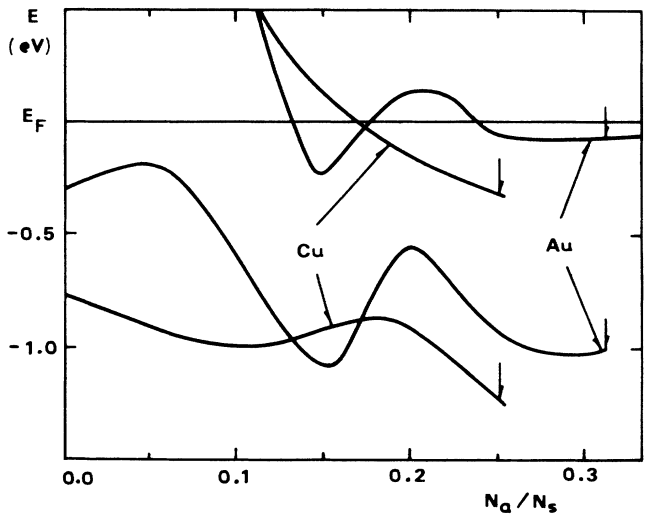

FIG. 15. Coverage dependences of the energies at the $\bar{\Gamma}$ point of bonding and antibonding bands between the SR1 of the substrate and the adlayer jellium state for the cesiated CU(001) and Au(001) surfaces. The coverage axis is scaled by the surface atomic density N_s of the corresponding substrate. Vertical arrows show the monolayer coverage.

IV. ADSORPTION-INDUCED DIPOLE MOMENT

According to the above discussion, the electrons of the alkali-metal adlayer are ionized to fill the most influential surface state or resonance (generally lying near the E_F) of the transition or noble metal substrates at the lower coverage. At the higher coverage, on the contrary, the adsorption electrons tend to distribute uniformly over their positive background region to form a neutral metallic bond within the overlayer. Such charge rearrangement, however, will certainly lead to the change of the surface barrier and thereby the work function.

As illustrated in Ref. 12, the adsorption dipole moment $p(N_a)$ is the key quantity to describe the rearrangement of the adsorption electrons. In Fig. 17, the curves of the p versus normalized adsorption coverage N_a/N_s for the above systems are shown. Even though these curves exhibit different behaviors in detail, generally they can be divided into two regimes by a coverage N_m, i.e., the con-

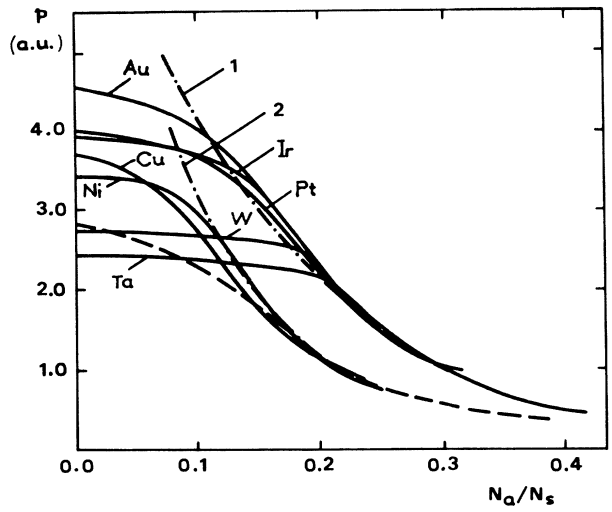

FIG. 17. Atomic dipole moment $p(N_a/N_s)$ of cesiated Cu, Ni, W, Ta, Ir, Pt, and Au (001) surfaces. The dashed line is reproduced from Ref. 6 obtained with the jellium-jellium model by Lang. Dotted-dashed lines are the fitted asymptotes (see text for details).

stant or slowly decreasing regime at the lower coverage ($N_a < N_m$), and the quickly decreasing regime at the higher coverage ($N_a > N_m$). These two regimes, however, correspond to the ionic and the polarized-metallic adlayer-substrate interaction, respectively. The coverage N_m depends on the substrate, and can be considered as the critical point where the adlayer-substrate interaction changes its character (Mott-like transition).

For the Cs/Ta(001) and Cs/W(001) systems, since the $\bar{\Gamma}$ d_{z^2} surface states of the Ta(001) and W(001) substrates are localized and hardly change their spatial distribution with the alkali-metal adsorption, the dipole moment (curves c and d) for these two systems are almost constant within a long-coverage range [0 to $N_m/N_s = 0.2$ (for Ta) and 0.18 (for W)]. That means each d_{z^2} SS of the Ta(001) [or W(001)] substrate can hold 0.2 (or 0.18) extra electrons. From the value of $p(0) = 2.4$ a.u., the average center $\langle Z_e \rangle$ of the $\bar{\Gamma}$ d_{z^2} SS (being equal to the center of the redistributed adsorption electrons at the zero-coverage limit, i.e.,

$$\langle Z_e \rangle = \lim_{N_a \to 0} \int_0^\infty (z - d/2)\rho(z)dz/N_a = D/2 - p(0)$$

is 1.6 a.u. for the Ta(001) surface. So the SS of the Ta(001) surface extends even more to the vacuum than that of the W(001) surface [the corresponding $\langle Z_e \rangle$ for W(001) is 1.3 a.u.].

The $p(N_a/N_s)$ for the cesiated Ir(001) and Pt(001) [curves (e) and (f)] are approximately coincident with each other in the whole submonolayer range since their SR1's are very similar. The $p(0)$ of the Cs/Ir(001) and Cs/Pt(001) systems are 3.9 and 4.0 a.u., respectively, so the average center of their SR1's lies almost just on the interface (i.e., $\langle Z_e \rangle \cong 0$). Since these SR1's extend considerably into the interior of the substrate, adsorption electrons will be strongly screened out when they intend to fill the SR1. Therefore, the ability of the SR1 to hold extra electrons is greatly reduced compared to that of the $\bar{p}$ d_{z^2} SS of the Ta(001) and W(001) substrates. As shown in Fig. 17, the knee points N_m/N_s for the Cs/Ir(001) and Cs/Pt(001) systems are about 0.12 and 0.10, respectively, far less than those of the Cs/Ta(001) and Cs/W(001) systems. Furthermore, because the spatial distribution of the SR1 is very sensitive to the adsorption, the curves for Ir and Pt have already decreased 10% within the range $N_a < N_m$. The dipole moment for the cesiated Ni(001) surface shows the same qualitative behavior as for the Cs/Ir(001) and Cs/Pt(001) also, but its N_m/N_s is only 0.08, since the SR1 of the Ni(001) surface is more concentrated in its spatial range.

Because the d bands of the noble-metal substrates are entirely occupied, the $p(N_a/N_s)$ for Cs/Cu(001) and Cs/Au(001) start to decrease from the very beginning of the alkali-metal deposition without explicit knee points. The curve is similar to that obtained by Lang from the jellium-jellium model,[6] which is also shown in Fig. 17 by the dashed line. The value of $p(0)$ for the Cs/Cu(001) and Cs/Au(001) systems are 3.7 and 4.5 a.u., respectively.

In Fig. 18(a), the $p(0)$ (circles) and $\langle Z_e \rangle$ (squares) are

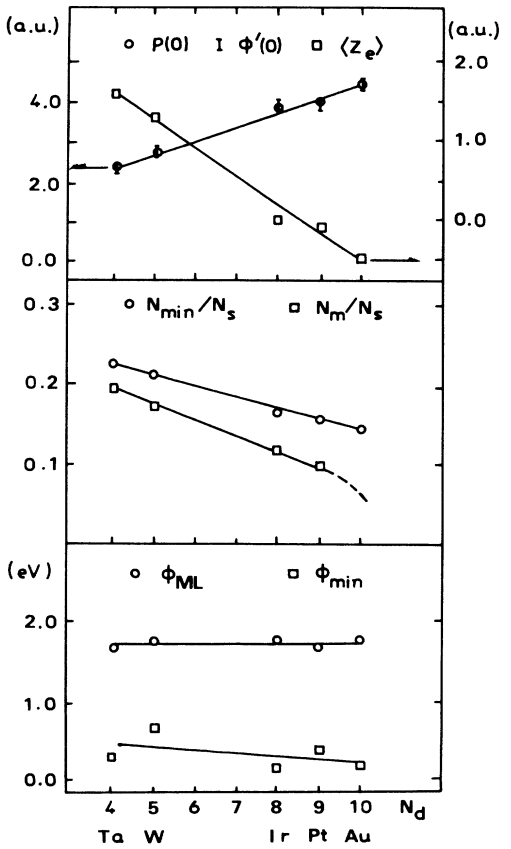

FIG. 18. Dependences on the N_d of the 5d series transition-metal substrates of (a) $p(0)$ (circles), $\phi'(0)$ (bars), and $\langle Z_e \rangle$ (squares); (b) N_m/N_s (squares) and $N_{\min}/N_s$ (circles); (c) $\phi_{\min}$ (squares) and ϕ_{ML} (circles).

plotted against the occupation number N_d of the $5d$ band of the substrates. It can be found that, the greater the N_d, the greater the $p(0)$, and the smaller the $\langle Z_e \rangle$. Therefore, the most effective surface state (or resonance) possesses less vacuum extension and can hold fewer extra electrons for the substrate closer to the end of the series. Subsequently, as shown in Fig. 18(b), the N_m/N_s (squares) decreases with the increasing N_d.

At the higher-coverage regime ($N_a > N_m$), however, to fill the surface state of the substrate further will be no longer energy favorable because of Coulombic repulsion between the gradually stacked electrons. The following adsorption electrons therefore are mainly rearranged into their intensified positive background to establish a metallic bond in the adlayer. As a result, the p decreases drastically with the growing coverage as shown in Fig. 18, similar to Lang's result obtained from the jellium-jellium model (dashed line). It thus can be assumed that at high coverage, transition-metal substrates influence the adlayer by their free electron bands. The detail of different d bands will be gradually screened out by the densified electrons in the adlayer and lose its predominate role as at the lower coverage. The adsorption electrons are so redistributed that the attractions by the substrate and the electrostatic depolarization field within the adlayer are balanced. Dramatically, the $p(N_a/N_s)$ curves fall into two asymptotes, each for one of the cesiated $3d$ and $5d$ transition series, after passing through corresponding critical points N_m. The decay of p with N_a shown by these asymptotes is faster than that expected by so-called Topping model [$p = p(0)/(1+kN_a^{-2/3})$] from the electrostatic depolarization interaction between point dipoles. Since there is no similarity between the present jellium description and the point-dipole model, this discrepancy is not surprising.

The two asymptotes given in Fig. 17 fit well with an exponential decay (dotted-dashed lines 1 and 2), $p(N_a/N_s) = 8.1 \exp(-\beta N_a/N_s)$ with $\beta = 6.9$ for $5d$ substrates and 9.5 for $3d$ substrates. Though the preexponential coefficient is in good agreement with the jellium thickness, corresponding to the fully ionized imaging dipole distance at the zero-coverage limit, a persuasive explanation for this exponential is still unknown. Since the decay is only in a short range of coverage, we are not very sure about the correctness of this exponential expression. However the success of the description of the work-function minimum and its approach to monolayer coverage (see next section) reveals that the depolarization that happens in this jellium model is a better description of the experiments than that given by the electrostatic interaction between point dipoles, as commonly accepted during the last decades.

V. WORK FUNCTION

In Fig. 19, the coverage dependences of the work function are drawn for all investigated systems. Very clearly, all these curves show the character for such alkali-metal–transition-metal chemisorption system. Related to the larger $p(0)$, the $\phi(N_a/N_s)$ shows a faster decrease for the substrate with larger N_d.

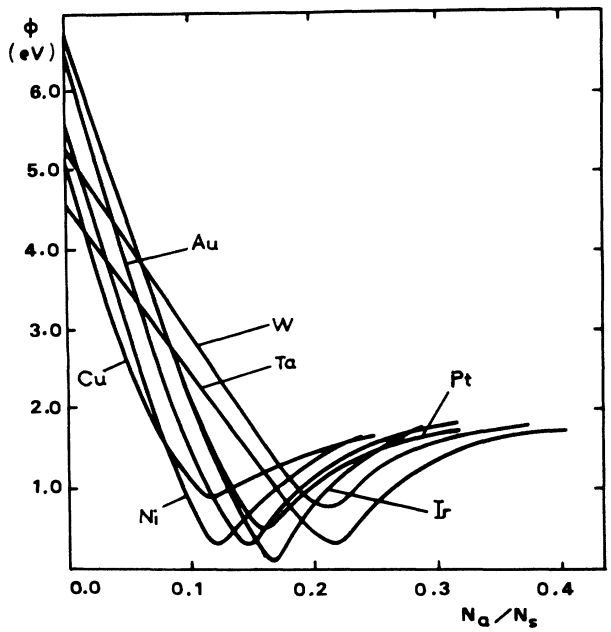

FIG. 19. Work function vs coverage for cesiated (001) surfaces of Cu, Ni, W, Ta, Ir, Pt, and Au. The coverage axis is scaled by the surface atomic density of the corresponding substrate.

In Table I, the often-cited quantities about the work function derived from Fig. 19 are given in comparison with related experimental values.[24] The best agreement between the present theory and the experiment is observed for $N_{\min}$, $\phi'(0)$, and ϕ_{ML}. As explained above, since the coverage for the work-function minimum N_m reflects the strength of the interaction between the local surface states and the adlayer s electrons, the present jellium-slab model is expected to give a good description. $\phi'(0)$ is related to the initial occupation of the empty local surface states. Since the LAPW method gives an accurate description of these surface states, it is not surprising to get this agreement. The monolayer coverage work-function ϕ_{ML} is mainly determined by the jellium layer, since the perturbation of the substrate has been screened in such high electron density. As in the case of the treatment of the work function of the alkali metal, the jellium model is expected to give good results. For the $\phi(0)$, the trend for different substrates agrees between present calculation and the experiment, e.g., the work function of Ta, Cu, and W is lower than that of another four substrates, but the present calculation gives results about 0.4–1.1 eV greater than that of the experiment. This deviation is from the fact that a three-layer slab is not thick enough to give work-function value.[13] Another discrepancy is for $\phi_{\min}$. Contrary to $\phi(0)$, the present theory gives results about 0.8–1.3 eV lower than that given by experiment. At least one of the reasons is that the contribution from the core Cs $5p$ electron to the surface dipole layer has not been taken into account in present jellium-slab model. Wimmer *et al.* reported that these core electrons polarize in the direction opposite

TABLE I. Theoretical and experimental results of some often-cited quantities about the work functions for cesiated transition-metal and noble-metal (001) surfaces.

		Cu	Ni	W	Ta	Ir	Pt	Au
$\phi(0)$ (eV)	theor.	5.1	5.7	5.4	4.6	6.6	6.7	6.4
	expt.	4.6	5.2	4.6	4.2	5.5	5.6	5.5
$\phi'(0)$ (D)	theor.	18.0	17.0	13.2	11.9	18.5	19.2	22.0
	expt.	20.5	22.0	13.0				
ϕ_{min} (eV)	theor.	0.9	0.3	0.7	0.3	0.2	0.4	0.2
	expt.	1.65	1.6	1.6		1.3		
N_{min}	theor.	0.2	0.21	0.22	0.21	0.23	0.22	0.20
(10^{15} cm^{-2})	expt.	0.21	0.22	0.24				
ϕ_{ML} (eV)	theor.	1.7	1.7	1.8	1.7	1.8	1.7	1.9
	expt.	2.07	2.0	1.9				

that of the valence electrons and contribute to the work function in the amount of about 0.5 eV.[7]

Changing to the same unit, (1 Debye $\cong$0.397 a.u.), the points of $\phi'(0)$ (bars) coincide entirely with those of $p(0)$ (circles) in Fig. 18(a). This indicates that the dipole contribution dominates the variation of the work function, and also provides an elegant support for the present model used at the low-coverage limit because, from Table I, the $\phi'(0)$ agrees with the experimental value very well.

In Fig. 18(b), the points of N_{min}/N_s (circles) for $5d$ series substrates is plotted. Similar to the N_m, N_{min}/N_s also decrease with the growing N_d. The points of ϕ_{ML} (circles) and ϕ_{min} (squares) with respect to the N_d are plotted in Fig. 18(c). Though the $\phi(0)$ varies more than 2 eV from 6.8 eV for Au(001) to 4.6 eV for Ta(001), the ϕ_{min} is almost the same (about 0.5 eV) for all systems independent of the substrates. The ϕ_{ML}, however, is also constant (about 1.8 eV) for all systems. This value is approximately equal to the work function of the clean Cs surface (2.0 eV). It implies that the work function is only determined by the adlayer itself at the very high coverage.

VI. SUMMARY AND CONCLUSION

In summary, we have investigated thoroughly the chemisorption systems consisting of a submonolayer alkali-metal (Cs) overlayer and various transition-metal or noble-metal substrates. The role of the surface states in the chemisorption process and other surface electronic properties have been elucidated.

1. The whole submonolayer adsorption range can be divided into an ionic regime at the lower coverage and a polarized-metallic regime at the higher coverage by a critical point N_m. This critical coverage N_m is substrate dependent and can be considered as the ability of the most influential SS or SR of the substrate to hold extra electrons.

2. At the lower coverage, the effect of the substrate on the alkali-metal adlayer is dominated by the most influential surface state (or resonance). The center of gravity of the most influential SS (or SR) shifts inward gradually when the species of the substrate atom go to the right of the period table through the transition series.

3. At the higher coverage, the influence of the localized substrate states is screened out. Adsorption electrons distribute uniformly over their intensified positive background to establish a polarized-metallic bond in the adlayer.

ACKNOWLEDGMENTS

This work was supported by the National Science Foundation of China under Grant No. 6881018. One of the authors (D.-S.W.) wishes to thank Professor A. J. Freeman of Northwestern University for helpful discussions and hospitality.

[1]K. H. Kingdon and I. Langmuir, Phys. Rev. **21**, 380 (1923); J. B. Taylor and I. Langmuir, *ibid.* **44**, 423 (1933).

[2]J. Hölzel and F. K. Schulte, *Work Function of Metals*, Vol. 85 of *Springer Tracts in Modern Physics* (Springer-Verlag, Berlin, 1979).

[3]H. P. Bonzel, Surf. Sci. Rep. **8**, 43 (1988).

[4]Z. Sidorski, Appl. Phys. A **33**, 213 (1984); Z. Sidorski and K. F. Wojciechowski, Acta. Phys. Pol. A **40**, 662 (1970).

[5]P. Soukiassian, R. Riwan, J. Lecante, E. Wimmer, S. R. Chubb, and A. J. Freeman, Phys. Rev. B **31**, 4911 (1985).

[6]N. D. Lang, Phys. Rev. B **12**, 4234 (1971).

[7]E. Wimmer, A. J. Freeman, J. R. Hiskes, and A. M. Karo, Phys. Rev. B **28**, 3074 (1983).

[8]S. R. Chubb, E. Wimmer, A. J. Freeman, J. R. Hiskes, and A. M. Karo, Phys. Rev. B **36**, 4112 (1987); J. Vac. Sci. Technol. A **5**, 695 (1987).

[9]H. Ishida and K. Terakura, Phys. Rev. B **36**, 4510 (1987).

[10]J. Cousty and R. Riwan, Europhys. Lett. **3**, 1119 (1987); J. Cousty, R. Riwan, P. Soukiassian, and F. Mila, J. Phys. C **19**, 2833 (1986).

[11]Ning Wang, Kailai Chen, and Ding-sheng Wang, Phys. Rev. Lett. **56**, 2759 (1986).
[12]Ru-qian Wu, Kai-Iai Chen, Ding-sheng Wang, and Ning Wang, Phys. Rev. B **38**, 3180 (1988).
[13]S. Ohnishi, A. J. Freeman, and E. Wimmer, Phys. Rev. B **29**, 5267 (1984).
[14]H. Krakauer, Phys. Rev. B **30**, 6834 (1984).
[15]R. L. Gerlach and T. N. Rhodin, Surf. Sci. **19**, 403 (1970).
[16]H. Krakauer, A. J. Freeman, and E. Wimmer, Phys. Rev. B **28**, 610 (1983); F. J. Arlinghaus, J. G. Gay, and J. R. Smith, *ibid.* **21**, 2055 (1980).
[17]E. Plummer and W. Eberhardt, Phys. Rev. B **20**, 1444 (1979).
[18]G. A. Somorjai, Catal. Rev. **7**, 87 (1972); S. M. Davis and G. A. Somorjai, Surf. Sci. **91**, 73 (1980); J. Catal. **67**, 371 (1981).
[19]R. D. Kelley and D. W. Goodman, in *The Chemical Physics of Solid Surface and Heterogeneous Catalysis,* edited by D. A. King and D. P. Woodruff (Elseviser, Amsterdam, 1982), Vol. 4, p. 427.
[20]Dingsheng Wang, A. J. Freeman, and H. Krakauer, Phys. Rev. B **26**, 1340 (1982).
[21]J. G. Gay, J. R. Smith, and F. J. Arlinghaus, Phys. Rev. Lett. **42**, 332 (1979); Phys. Rev. B **21**, 2201 (1980).
[22]E. Euceda, D. M. Bylander, L. Kleinman, and K. Mednic, Phys. Rev. B **27**, 659 (1983).
[23]S. A. Lindgren and L. Wallden, Solid State Commun. **28**, 282 (1978); **34**, 671 (1980).
[24]C. A. Papageorgopoulos, Phys. Rev. B **25**, 3740 (1982); Surf. Sci. **52**, 40 (1975); **39**, 283 (1973).